Environmental Science & Technology

ARTICLE

pubs.acs.org/est

All-Time Releases of Mercury to the Atmosphere from Human Activities

David G. Streets,[†,*] Molly K. Devane,[†] Zifeng Lu,[†] Tami C. Bond,[‡] Elsie M. Sunderland,[§] and Daniel J. Jacob[∥]

[†]Decision and Information Sciences Division, Argonne National Laboratory, Argonne, Illinois, United States

[‡]Department of Civil & Environmental Engineering, University of Illinois at Urbana−Champaign, Urbana, Illinois, United States

[§]Department of Environmental Health, Harvard School of Public Health, Boston, Massachusetts, United States

[∥]School of Engineering and Applied Science, Harvard University, Cambridge, Massachusetts, United States

Supporting Information

ABSTRACT: Understanding the biogeochemical cycling of mercury is critical for explaining the presence of mercury in remote regions of the world, such as the Arctic and the Himalayas, as well as local concentrations. While we have good knowledge of present-day fluxes of mercury to the atmosphere, we have little knowledge of what emission levels were like in the past. Here we develop a trend of anthropogenic emissions of mercury to the atmosphere from 1850 to 2008—for which relatively complete data are available—and supplement that trend with an estimate of anthropogenic emissions prior to 1850. Global mercury emissions peaked in 1890 at 2600 Mg yr^{-1}, fell to 700−800 Mg yr^{-1} in the interwar years, then rose steadily after 1950 to present-day levels of 2000 Mg yr^{-1}. Our estimate for total mercury emissions from human activities over all time is 350 Gg, of which 39% was emitted before 1850 and 61% after 1850. Using an eight-compartment global box-model of mercury biogeochemical cycling, we show that these emission trends successfully reproduce present-day atmospheric enrichment in mercury.

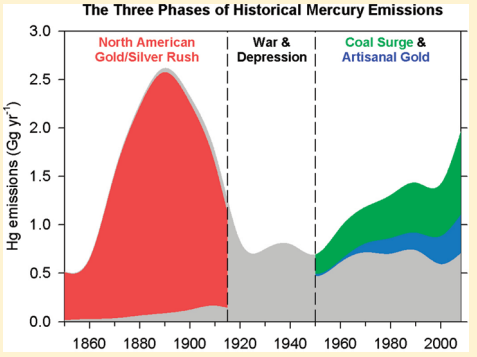

INTRODUCTION

Mercury (Hg) is a natural element found everywhere in the Earth's lithosphere. It is emitted naturally from the lithosphere to the atmosphere as gaseous elemental Hg^0 through processes of erosion and volcanism. The atmospheric lifetime of Hg^0 against deposition is ∼1 year, allowing transport on global scale.[1−4] Deposited Hg cycles through the surface environment in oceans and soils, can be re-emitted to the atmosphere, and is eventually buried in ocean sediments or stable terrestrial reservoirs. Human activity, including fossil-fuel combustion, mining, and industrial production, has greatly augmented the natural flux of Hg from the lithosphere to the atmosphere and from there to the surface environment. Present-day anthropogenic emissions are estimated to be about 2000 Mg yr^{-1}, as compared to 500 Mg yr^{-1} for the natural geogenic emissions.[5−9] The resulting accumulation of Hg in the environment has been documented from analysis of deposits in snow,[4,10] ice cores,[11] lake sediments,[12−15] and peat cores.[16,17]

Humans have disrupted the natural Hg cycle throughout their history in pursuit of riches, useful metals, and energy. It was 5000 years ago when humans first began digging into the Earth's crust to extract gold, silver, copper, coal, and other materials, all of which came laced with Hg. Since those ancient days, ever-increasing amounts of ever-varying materials have been extracted and refined, and large quantities of Hg have been liberated in the process. The time scale for return of anthropogenic Hg to sediments has been estimated to be ∼2000 years.[18,19] The accumulation of Hg in the global environment thus represents the legacy of historical emissions, with continuous augmentation from present-day human activities. Balancing the sources, sinks, and fluxes of Hg in different parts of the world at different times remains a modeling challenge, however,[18−25] and lack of knowledge of historical man-made contributions has inhibited progress.

DATA AND METHODS

The purpose of this present work is to develop an estimate of the total amount of Hg released to the atmosphere due to human activities from the dawn of civilization until 2008, the most recent year for which activity data are available. For the period 1850−2008, we present detailed decadal trends for each major source type and each region of the world. Fourteen source types are included: copper, zinc, and lead smelting; artisanal and large-scale gold production; iron and steel manufacturing (separately); silver production; mercury production; cement manufacturing; caustic soda manufacturing (at chlor-alkali plants); and the combustion of coal, oil, and waste. We do not include emissions from biofuel or open biomass burning, as these represent a recycling of Hg previously deposited in the surface environment. Emissions are calculated for

Received: August 8, 2011
Accepted: November 9, 2011
Revised: October 20, 2011
Published: November 09, 2011

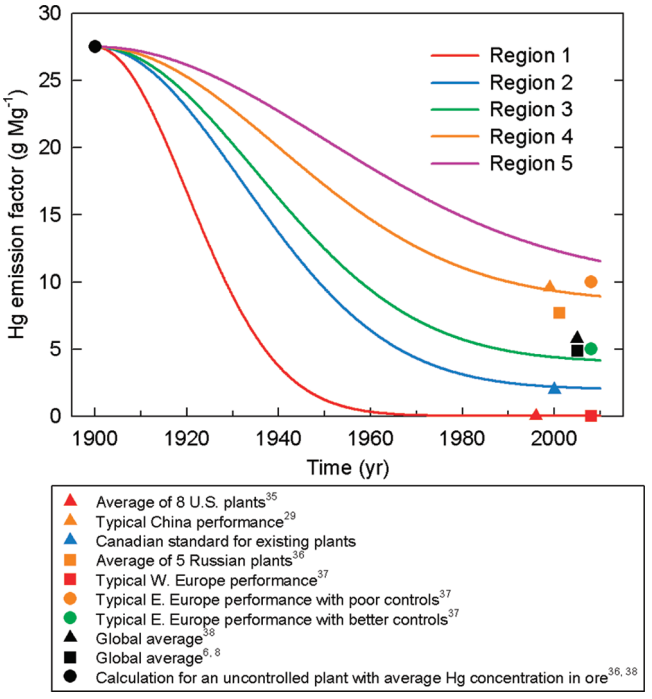

Figure 1. Time development of Hg emission factors for Cu smelters in five world regions. Each world region is comprised of countries with similar levels of technology development, ranging from most developed (Region 1) to least developed (Region 5). The composition of these regions is provided in Table S1 of the SI.

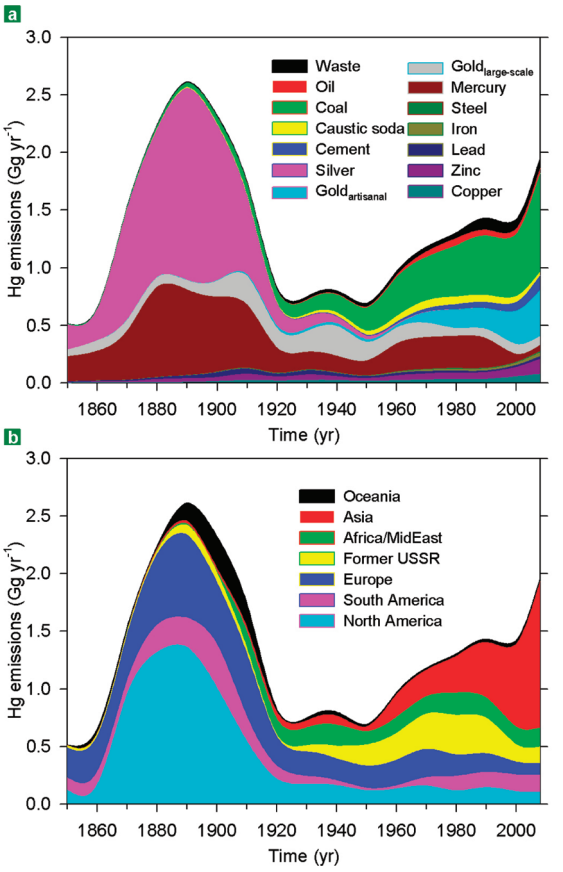

Figure 2. Trends in Hg emissions by (a) source type and (b) world region.

17 world regions (defined in Table S1 of the Supporting Information (SI)). The method integrates our previous work on historical and future emissions[26−28] with our work on Hg emissions.[9,29−31] For the 11 industrial commodities, the assembly of historical production levels between 1850 and 2008 is documented in the SI. For the three combustion-related emissions, the activity levels are the same as used in previous work,[26−28] disaggregated into 144 sector/fuel/technology combinations (see Table 3 of ref 28.).

A major challenge is to develop a representation of the time-varying Hg emission factors associated with each industrial activity. We have developed a dynamic representation of emission factors since 1850 to reflect the transition from old, small-scale, uncontrolled processes to modern, large-scale processes with emission controls. We know that materials production has grown year-by-year—sometimes dramatically—but at the same time process technology has improved and pollution controls have been adopted. So the resulting level of emissions at any given time reduces to a competition between production growth and technology improvement.

We use the following transformed normal distribution function to estimate the variation of Hg emission factors over time:

$$y_{r,p,t} = (a_{r,p} - b_{r,p})e^{(-t^2/2s_{r,p}{}^2)} + b_{r,p}$$

where $y_{r,p,t}$ = emission factor in region r for process p in year t (g Mg^{-1}); $a_{r,p}$ = pre-1850 emission factor (g Mg^{-1}) in region r for process p; $b_{r,p}$ = best emission factor achieved in region r for process p today (g Mg^{-1}); and $s_{r,p}$ = shape parameter of the curve for region r and process p.

The use of such sigmoid curves to simulate the dynamics of technology change has been previously applied to energy and emission control technology,[32] carbon sequestration,[33] and automobile technology.[34] We have previously demonstrated the use of this technique in estimating both historical[26] and future[28] emissions. By selecting values of the parameters a, b, and s to correspond to the known or inferred time development pathway of relevant technologies, we can estimate the values of emission factor y at any point in time. Parameter values where this technique was used are provided in Table S2 of the SI.

Figure 1 illustrates the use of this technique for estimating Hg emission factors for copper smelters. Note that we use five world regions to represent different emission factor trajectories. Each world region is comprised of countries with similar levels of technology development, ranging from most developed (Region 1) to least developed (Region 5). The composition of these regions is provided in Table S1 of the SI. Emission factors for each world region were determined from a review of reported emission rates in representative countries[6,8,29,35−38] and used to anchor each trajectory. Table S3 of the SI presents and documents emission factor ranges for each industrial activity for 1850, 1930, and 2008 and provides citations for the studies used in the development of the emission factor curves. The procedure for combustion sources is different and follows previous work[26,28] in that unique emission factors are developed for each of the 144 sector/fuel/technology combinations, and transitions from simple to advanced systems are determined by technology shifts.

RESULTS AND DISCUSSION

Historical anthropogenic Hg emission trends from 1850 to 2008 are shown in Figure 2, disaggregated by source type (upper)

and world region (lower); here we aggregate emissions into seven super-regions (defined in Table S1 of the SI). We calculate that global Hg emissions peaked in 1890 at 2600 Mg yr^{-1}. This was mainly due to extensive production of gold (Au) and silver (Ag) and production of the Hg that was used to extract them via amalgamation; our results for this period are in good agreement with previous work.[39,40] Emissions then declined rapidly and remained relatively constant at 700−800 Mg yr^{-1} in the interwar years. After 1950, emissions grew again, driven mainly by growth in coal combustion and, lately, artisanal Au production, rising to 2000 Mg yr^{-1} in 2008. Present-day values are consistent with previous work,[6−9] as shown in Table S4 of the SI. The regional emission trends show that North America and Europe were the dominant emitting regions in the 19th century, but emphasis shifted initially to Russia and then sharply to Asia after 1950. We estimate that Asia was responsible for 64% of global Hg emissions in 2008.

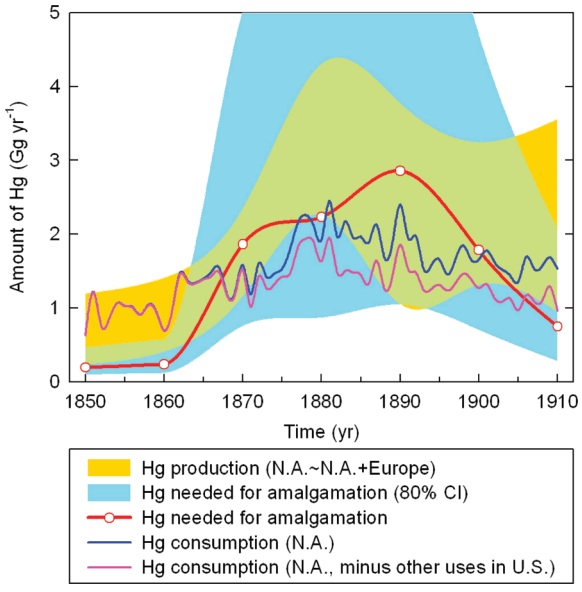

Figure 3. Estimates of Hg consumed in North America in the 19th century to extract Au/Ag.

We follow the methodology used previously for Hg emissions from power plants in China[31] to determine uncertainties in the emission estimates. All input parameters and their corresponding probability distributions were incorporated into a Monte Carlo framework with Crystal Ball software and 10 000 simulations performed. For activity rates we assumed normal distributions with time-, region-, and sector-dependent uncertainties, based on previous work.[26,30] Measurements of emission factors, if they existed, were applied directly in our model; and, if measurements were not available, probability distributions were based on expert judgment. For the emission estimates that follow, we present lower and upper bounds around the central estimate that correspond to an 80% confidence interval (CI), meaning that, based on the underlying distributions, the probability of emissions being outside the stated range is less than 20%. Figure S1 of the SI shows the uncertainty range of the historical global Hg emissions. The range of uncertainty is large before 1910 (lower bounds varying between −30% and −45% and upper bounds varying between +65% and +110%, depending on the year), decreasing to a relatively stable level after 1920 (−30% to +60%). Our modern-day uncertainty range is similar to estimates given by Pacyna et al.[8] SI Figure S1 also shows that the largest contributors to total variance are the emission factor for Au/Ag production before 1940 and the emission factor for coal combustion after 1940.

Because of the large contribution of the 19th century peak and its relatively high degree of uncertainty, we have investigated the situation in North America (the "Gold Rush") in detail. The red line in Figure 3 shows our estimate of the amount of Hg needed to extract the reported amounts of Au and Ag produced, assuming that amalgamation began to be phased out after 1880 in favor of cyanidation. We also show the range of uncertainty (blue) caused by uncertainties in the Au/Ag production data and the implied Hg emission factor. Because considerable amounts of Hg were exported from Spain, Italy, and Slovenia to Mexico, we know that the amount of Hg available lies somewhere in the range (yellow) bounded by production in North America (N.A.) and the

Table 1. Cumulative Commodity Production Amounts and Associated Hg Emissions[a]

material	pre-1850		1850−2008		all-time to 2008	
	production (Tg)	emissions (Mg)	production (Tg)	emissions (Mg)	production (Tg)	emissions (Mg)
copper	45	1240	547	3410	592	4650
zinc	50	3750	403	6520	453	10 300
lead	55	2400	268	3590	323	5990
iron	330	20	32 900	1110	33 300	1130
steel	∼0	∼0	44 200	388	44200	388
mercury	0.229	41 700	0.720	53 300	0.949	95 000
gold, large-scale	∼0	∼0	0.145	20 600	0.145	20 600
gold, artisanal	0.016	8200	0.025	10 200	0.041	18 400
silver	0.276	78 700	1.17	67 300	1.45	146 000
cement	∼0	∼0	61 200	3000	61 200	3000
caustic soda	∼0	∼0	1710	4240	1710	4240
coal	2900	868	319 000	33 900	322 000	34 800
oil	∼0	∼0	312 000	2620	312 000	2620
waste	∼0	∼0	2310	5310	2310	5310
total		137 000		215 000		352 000

[a] Values are rounded to no more than three significant digits, consistent with the level of confidence.

combined production in N.A. and Europe. Our trend line lies for the most part within the overlapping range (green) of uncertainties in Hg availability and Hg requirement. Actual Hg consumption data for N.A. are not known with confidence, but we show annual consumption values reported for N.A. and for N.A. minus the amounts of Hg that were used for purposes other than amalgamation in the U.S.[41] (These other uses are not known for Canada and Mexico.) We believe that the consumption statistics are too low after 1865 compared to both production values and the inferred requirements for amalgamation; we attribute this to underestimation or even omission of imported Hg from Europe. Sources of uncertainty in these historical data are: other uses of mercury (medicine and paint), stockpiling of cheap Hg for later use when prices rise, and timing of the replacement of amalgamation with cyanidation in Mexico and Canada.

Another issue is the amount of Hg lost per kg of Au/Ag produced, which we set at 1.3 kg. Previous recommendations for this ratio have ranged between 0.75 and 1.5,[40,42] and Nriagu[43] suggested a range of values from 0.85−4.1, depending on the richness of the ore (the richer the ore, the more Hg need for extraction). It is possible that in the early periods of Au/Ag mining in North America, richer ores were mined and more Hg was used. To test this possibility, we calculated the ratios of apparent Hg consumption to the amount of Hg required. Values are: 4.02 (1850s), 1.37 (1860s), 1.00 (1870s), 0.89 (1880s), 0.88 (1890s), and 1.15 (1900s). These values are thus consistent with declining ore richness.[43] Our emission estimates for this period are in good agreement with previous estimates,[39,40] and therefore we have confidence in the size and timing of the 19th century peak in Hg emissions. Figure S2 of the SI shows the full trend of Hg emissions in North America.

Integrating under the trend curve (Figure 2), we calculate that a cumulative total of 215 (−34% to +74%) Gg of Hg were released to the atmosphere from human activities between 1850 and 2008. Table 1 shows that emissions during this period were dominated by Ag production (31%), Hg production (25%), and coal combustion (16%). The dominant regions were North America (32%), Europe (24%), and Asia (13%).

We also conducted a review of materials production and fuel combustion for the period from when humans first began to extract metals (ca. 3000 BC) until 1850. There are good estimates for the large contributions of Ag mining in South and Central America in the 16th−18th centuries.[42−46] We also consulted a wide variety of other historical sources (see the SI). We estimate that about 137 Gg of Hg were released prior to 1850. It is not possible to do a formal uncertainty analysis for this value, but we believe confidence is on the order of −50% to +300%. This pre-1850 amount of Hg is dominated by Ag production in Spanish America (58% of total) and production of the Hg needed to extract it (30%). Combining the pre-1850 and post-1850 values leads to the conclusion that cumulative, all-time releases of Hg to the atmosphere up to 2008 have been about 350 Gg.

For anthropogenic emissions since 1850 we are able to develop speciated emission trends using speciation factors that we have documented in previous work.[9,29,30] Figure 4 shows that the share of Hg^0 in total Hg emissions has declined from 80% in 1850 to 55% today. Nevertheless, emissions of Hg^0 have grown steadily in the modern era, from 420 Mg yr^{-1} in 1950 to 1080 Mg yr^{-1} in 2008, due to worldwide economic and industrial development.

The emissions that we have calculated are direct releases, that is to say, injection of Hg directly into the atmosphere from thermal processes. In addition, there have been comparable quantities of anthropogenic Hg directly released from these

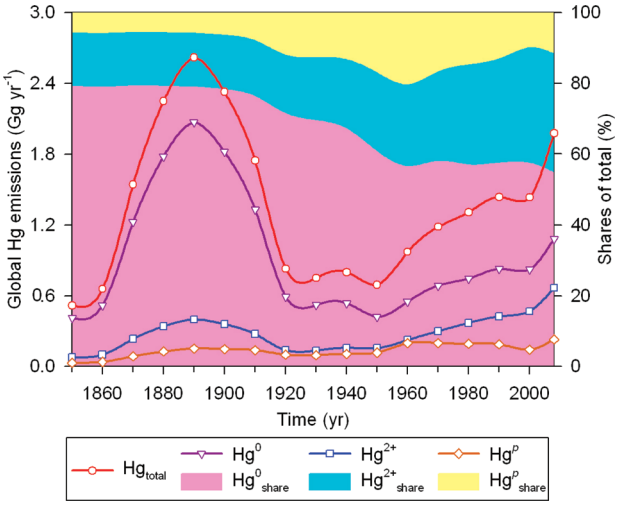

Figure 4. Trends in speciated emissions of Hg: absolute magnitude (lines) and shares of total (shading).

same industrial activities as liquid and solid waste streams that have been deposited locally to land surfaces and water bodies. It is more difficult to quantify these pools of Hg, but they may be amenable to estimation based on some of our results, such as the total commercial production of Hg over time, the amounts of raw ore and fuel processed, and the amounts of Hg captured by emission control devices. As one example, we estimate in this work that 720 Gg of Hg were produced commercially between 1850 and 2008 (Table 1), of which 340 Gg were used to extract Au/Ag. This implies that about 380 Gg of Hg have been used for other purposes—in other industrial processes or in the manufacture of products. This large pool of unaccounted Hg is likely sequestered in landfills and other localized waste repositories. Nevertheless, it will eventually be released on time scales faster than the natural geogenic sources and therefore should be accounted for in biogeochemical models. Any changes to the availability of these nonatmospheric repositories of man-made Hg through activities such as dredging and waste combustion could liberate large quantities of Hg to the atmosphere and biosphere.

Using the historical atmospheric emissions inventory developed here we are able to construct a temporally resolved simulation of how various biogeochemical reservoirs have changed in response to anthropogenically mobilized Hg. To do this, we developed an eight-compartment global box-model that is based on current estimates of global budgets.[18,22−24] The model includes three fast-cycling surface reservoirs (the atmosphere, the surface mixed-layer of the ocean, and a rapidly responding terrestrial compartment that includes vegetation, sea-ice, snowpacks, and labile organic carbon pools), two intermediate compartments that respond on the order of decades (intermediate ocean and slow terrestrial reservoir), two deep reservoirs that respond on the order of centuries (deep ocean and armored soil pool), and the large mineral reservoir of Hg.

We assume that the mass flows between compartments in this eight-box model are governed by first-order processes having the same rate constants in the preindustrial period and the present. These rate constants are specified from global models of Hg cycling in the atmosphere,[24] terrestrial systems,[22] surface ocean,[23] and intermediate and deep ocean.[18] We first run the model to steady state using a geogenic emissions value[6] of 200 Mg yr^{-1}. We then conduct a time-dependent simulation between 1450 and 2008 using the historical emissions presented here. Biomass burning is specified

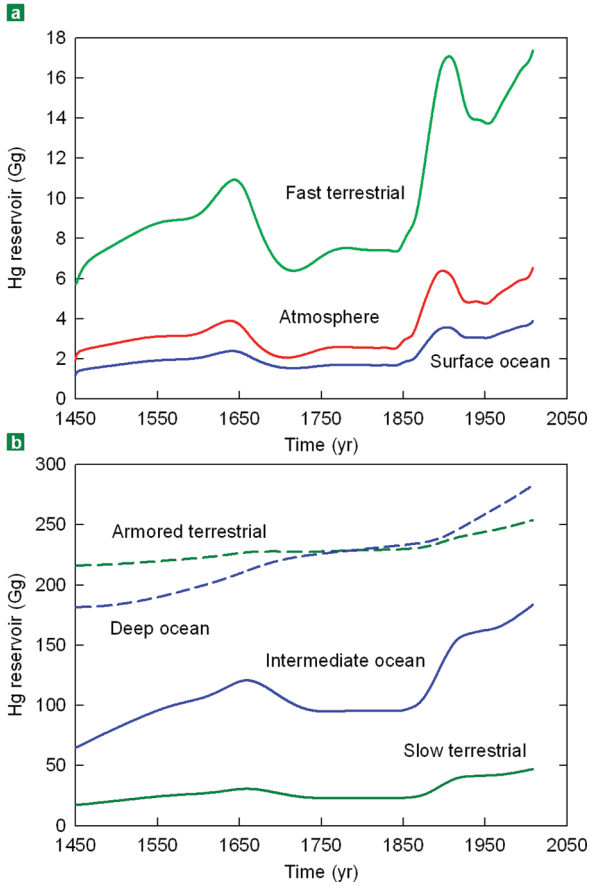

Figure 5. Modeled, time-dependent accumulation of anthropogenic Hg in global biogeochemical reservoirs.

as a constant value of 300 Mg yr^{-1} between 1450 and the present. For anthropogenic emissions occurring before 1850, we divide the total releases (137 Gg) into a peak emissions period spanning 200 years (80% of total releases) to represent Ag mining in South and Central America between 1450 and 1650.[43,46] We assume the remaining fraction of pre-1850 anthropogenic emissions (20%) was released at a constant rate between 1650 and 1850.

Figure 5 shows the resulting modeled trends in the fast, intermediate, and slowly responding Hg reservoirs between 1450 and present. Results show that the present-day atmosphere has been enriched in Hg by a factor of 3.9 (range of 3.2−6.9 based on the low and high emission estimates shown in Figure S1 of the SI), which is in excellent agreement with archival records of deposition in ice and sediments.[11,39] Fast-cycling terrestrial and ocean surface reservoirs closely track temporal trends in atmospheric concentrations and historical emissions, peaking in the early 1600s and 1800s due to Au and Ag mining and rising again after 1950 due to the large increases in coal combustion.

Slow terrestrial and intermediate ocean Hg concentrations reflect a longer time history of anthropogenic inputs, because the lifetime of Hg in these reservoirs is on the order of decades (Figure 5). In slow terrestrial and subsurface ocean reservoirs it is possible to distinguish among peaks occurring in the 1600s due to Ag mining in South and Central America and the rise in emissions in 1850 to present day, though the local minimum in the early 1900s is not visible. Present-day enrichment of these reservoirs from anthropogenic sources is between 270−280% relative to pre-1450 levels. This is higher than previous model estimates for the intermediate ocean[18,25] that could not consider releases prior to 1850 and the fully resolved time history of anthropogenic emissions presented here. Considerable accumulation of historical anthropogenic Hg is evident in the deep ocean (>100 Gg since 1450) compared to <1 Gg in the armored soil pool because of the large sink of mercury from the surface and intermediate ocean through particle settling. Because of the long lifetime of Hg in the deep ocean (many centuries) and armored terrestrial pools, these reservoirs will continue to slowly rise over time, even with declines in future emissions.

A recent analysis of worldwide trends in Hg concentrations in air and wet deposition[47] showed a 20−38% decline in atmospheric Hg concentrations from 1996 to 2009 at long-term monitoring stations in the Northern and Southern Hemisphere. A declining trend was also reported at the Mace Head baseline station in Ireland[48] and at the Alert station in the Canadian Arctic,[49] though the magnitude of the change at Alert was smaller. These measurement trends are in apparent conflict with the increasing trends in primary anthropogenic Hg^0 emissions presented here (Figure 4).

Slemr et al.[47] postulated that the recent decline in atmospheric Hg could be due to declines in re-emission of Hg from surface ocean and soil reservoirs. Our geochemical box-model analysis shows a 1900−1950 decline of atmospheric concentrations following the late 19th century maximum in emissions, but a post-1950 increase driven by growing emissions (Figure 5). Although there is uncertainty regarding the time scales for re-emission and transfer to stable geochemical reservoirs, the trend of increasing anthropogenic emissions shown in Figure 2 is incompatible with a decline in Hg in the surface reservoirs. The observed atmospheric decline could possibly reflect a suppression of re-emission from the surface reservoirs or an increase in atmospheric oxidant concentrations, but there is no independent evidence for such effects.

One possible explanation for the observed atmospheric decline is the legacy of Hg in commercial products (batteries, thermometers, switches, etc.). Production of these Hg-containing products peaked in the late 20th century (ca. 1970) and has been declining since then. This Hg eventually enters the environment through incineration, wastewater, or leakage from landfills and other solid waste repositories. Our inventory accounts for incineration but not the other modes of disposal. As pointed out above, the quantities involved are large, and there is little knowledge of how rapidly they could enter the environment and be emitted to the atmosphere. Better understanding is needed of the processes and time scales involved.

■ ASSOCIATED CONTENT

Supporting Information. (1) Development of production data, 1850−2008; (2) Development of production data, pre-1850; (3) References used for production data; (4) Regional definitions (Table S1); (5) Parameter values used in the sigmoid function computation of time-varying Hg emissions factors (Table S2); (6) Hg emission factors for industrial processes (Table S3); (7) Comparison of Hg emission estimates for recent years (Table S4); (8) Uncertainty ranges (Figure S1); (9) Historical trend in North American Hg emissions (Figure S2). This material is available free of charge via the Internet at http://pubs.acs.org.

■ AUTHOR INFORMATION

Corresponding Author

*Phone: (630) 252-3448; fax: (630) 252-6500; e-mail: dstreets@anl.gov.

■ ACKNOWLEDGMENT

Work at Argonne National Laboratory was supported by the U.S. Department of Energy. Argonne National Laboratory is operated by UChicago Argonne, LLC, under Contract No. DE-AC02-06CH11357 with the U.S. Department of Energy. Work at Harvard University was supported by the U.S. National Science Foundation. E.M.S. acknowledges new investigator support from the HSPH-NIEHS Center for Environmental Health.

■ REFERENCES

(1) Fitzgerald, W. F.; Engstrom, D. R.; Mason, R. P.; Nater, E. A. The case for atmospheric mercury contamination in remote areas. *Environ. Sci. Technol.* **1998**, *32*, 1–7.

(2) Durnford, D.; Dastoor, A.; Figueras-Nieto, D.; Ryjkov, A. Long range transport of mercury to the Arctic and across Canada. *Atmos. Chem. Phys.* **2010**, *10*, 6063–6086.

(3) Temme, C.; Einax, J. W.; Ebinghaus, R.; Schroeder, W. H. Measurements of atmospheric mercury species at a coastal site in the Antarctic and over the South Atlantic Ocean during polar summer. *Environ. Sci. Technol.* **2003**, *37*, 22–31.

(4) Loewen, M.; Kang, S.; Armstrong, D.; Zhang, Q.; Tomy, G.; Wang, F. Atmospheric transport of mercury to the Tibetan Plateau. *Environ. Sci. Technol.* **2007**, *41*, 7632–7638.

(5) *Mercury Fate and Transport in the Global Atmosphere*; Pirrone, N., Mason, R., Eds.; Springer: New York, 2009.

(6) Pirrone, N.; Cinnirella, S.; Feng, X.; Finkelman, R. B.; Friedli, H. R.; Leaner, J.; Mason, R.; Mukherjee, A. B.; Stracher, G. B.; Streets, D. G.; Telmer, K. Global mercury emissions to the atmosphere from anthropogenic and natural sources. *Atmos. Chem. Phys.* **2010**, *10*, 5951–5964.

(7) Pacyna, E. G.; Pacyna, J. M.; Steenhuisen, F.; Wilson, S. Global anthropogenic mercury emission inventory for 2000. *Atmos. Environ.* **2006**, *40*, 4048–4063.

(8) Pacyna, E. G.; Pacyna, J. M.; Sundseth, K.; Munthe, J.; Kindbom, K.; Wilson, S.; Steenhuisen, F.; Maxson, P. Global emission of mercury to the atmosphere from anthropogenic sources in 2005 and projections to 2020. *Atmos. Environ.* **2010**, *44*, 2487–2499.

(9) Streets, D. G.; Zhang, Q.; Wu, Y. Projections of global mercury emissions in 2050. *Environ. Sci. Technol.* **2009**, *43*, 2983–2988.

(10) Lahoutifard, N.; Sparling, M.; Lean, D. Total and methyl mercury patterns in Arctic snow during springtime at Resolute, Nunavut, Canada. *Atmos. Environ.* **2005**, *39*, 7597–7606.

(11) Schuster, P. F.; Krabbenhoft, D. P.; Naftz, D. L.; Cecil, L. D.; Olson, M. L.; Dewild, J. F.; Susong, D. D.; Green, J. R.; Abbott, M. L. Atmospheric mercury deposition during the last 270 years: A glacial ice core record of natural and anthropogenic sources. *Environ. Sci. Technol.* **2002**, *36*, 2303–2310.

(12) Phillips, V. J. A.; Louis, V. L., St.; Cooke, C. A.; Vinebrooke, R. D.; Hobbs, W. O. Increased mercury loadings to western Canadian Alpine lakes over the past 150 years. *Environ. Sci. Technol.* **2011**, *45*, 2042–2047.

(13) Ribeiro Guevara, S.; Meili, M.; Rizzo, A.; Daga, R.; Arribére, M. Sediment records of highly variable mercury inputs to mountain lakes in Patagonia during the past millennium. *Atmos. Chem. Phys.* **2010**, *10*, 3443–3453.

(14) Yang, H.; Battarbee, R. W.; Turner, S. D.; Rose, N. L.; Derwent, R. G.; Wu, G.; Yang, R. Historical reconstruction of mercury pollution across the Tibetan Plateau using lake sediments. *Environ. Sci. Technol.* **2010**, *44*, 2918–2924.

(15) Mast, M. A.; Manthorne, D. J.; Roth, D. A. Historical deposition of mercury and selected trace elements to high-elevation National Parks in the western U.S. inferred from lake-sediment cores. *Atmos. Environ.* **2010**, *44*, 2577–2586.

(16) Madsen, P. P. Peat bog records of atmospheric mercury deposition. *Nature* **1981**, *293*, 127–130.

(17) Givelet, N.; Roos-Barraclough, F.; Shotyk, W. Predominant anthropogenic sources and rates of atmospheric mercury accumulation in southern Ontario recorded by peat cores from three bogs: Comparison with natural "background" values (past 8000 years). *J. Environ. Monit.* **2003**, *5*, 935–949.

(18) Sunderland, E. M.; Mason, R. P. Human impacts on open ocean mercury concentrations. *Global Biogeochem. Cycles* **2007**, *21*, GB4022, [Online early access] DOI: 10.1029/2006GB002876.

(19) Selin, N. E.; Jacob, D. J.; Yantosca, R. M.; Strode, S.; Jaeglé, L.; Sunderland, E. M. Global 3-D land-ocean-atmosphere model for mercury: Present-day versus preindustrial cycles and anthropogenic enrichment factors for deposition. *Global Biogeochem. Cycles* **2008**, *22*, GB2011, [Online early access] DOI: 10.1029/2007GB003040.

(20) Lamborg, C. H.; Fitzgerald, W. F.; Damman, A. W. H.; Benoit, J. M.; Balcom, P. H.; Engstrom, D. R. Modern and historic atmospheric mercury fluxes in both hemispheres: Global and regional mercury cycling implications. *Global Biogeochem. Cycles* **2002**, *16*, 1104, [Online early access] DOI: 10.1029/2001GB001847.

(21) Selin, N. E.; Jacob, D. J.; Park, R. J.; Yantosca, R. M.; Strode, S.; Jaeglé, L.; Jaffe, D. Chemical cycling and deposition of atmospheric mercury: Global constraints from observations. *J. Geophys. Res.* **2007**, *112*, D02308, [Online early access] DOI: 10.1029/2006JD007450.

(22) Smith-Downey, N. V.; Sunderland, E. M.; Jacob, D. J. Anthropogenic impacts on global storage and emissions of mercury from terrestrial soils: Insights from a new global model. *J. Geophys. Res.* **2010**, *115*, G03008, [Online early access] DOI: 10.1029JG001124.

(23) Soerensen, A. L.; Sunderland, E. M.; Holmes, C. D.; Jacob, D. J.; Yantosca, R. M.; Skov, H.; Christensen, J. H.; Strode, S. A.; Mason, R. P. An improved global model for air-sea exchange of mercury: High concentrations over the North Atlantic. *Environ. Sci. Technol.* **2010**, *44*, 8574–8580.

(24) Holmes, C. D.; Jacob, D. J.; Corbitt, E. S.; Mao, J.; Yang, X.; Talbot, R.; Slemr, F. Global atmospheric model for mercury including oxidation by bromine atoms. *Atmos. Chem. Phys.* **2010**, *10*, 12037–12057.

(25) Strode, S.; Jaeglé, L.; Emerson, S. Vertical transport of anthropogenic mercury in the ocean. *Global Biogeochem. Cycles* **2010**, *24*, GB4014, [Online early access] DOI: 10.1029/2009GB003728.

(26) Bond, T. C.; Bhardwaj, E.; Dong, R.; Jogani, R.; Jung, S.; Roden, C.; Streets, D. G.; Trautmann, N. M. Historical emissions of black and organic carbon aerosol from energy-related combustion, 1850−2000. *Global Biogeochem. Cycles* **2007**, *21*, GB2018, [Online early access] DOI: 10.1029/2006GB002840.

(27) Lamarque, J.-F.; Bond, T. C.; Eyring, V.; Granier, C.; Heil, A.; Klimont, Z.; Lee, D.; Liousse, C.; Mieville, A.; Owen, B.; Schultz, M. G.; Shindell, D.; Smith, S. J.; Stehfest, E.; Van Aardenne, J.; Cooper, O. R.; Kainuma, M.; Mahowald, N.; McConnell, J. R.; Naik, V.; Riahi, K.; van Vuuren, D. P. Historical (1850−2000) gridded anthropogenic and biomass burning emissions of reactive gases and aerosols: Methodology and application. *Atmos. Chem. Phys.* **2010**, *10*, 7017–7039.

(28) Streets, D. G.; Bond, T. C.; Lee, T.; Jang, C. On the future of carbonaceous aerosol emissions. *J. Geophys. Res.* **2004**, *109*, D24212, [Online early access] DOI: 10.1029/2004JD004902.

(29) Streets, D. G.; Hao, J.; Wu, Y.; Jiang, J.; Chan, M.; Tian, H.; Feng, X. Anthropogenic mercury emissions in China. *Atmos. Environ.* **2005**, *39*, 7789–7806.

(30) Wu, Y.; Wang, S.; Streets, D. G.; Hao, J.; Chan, M.; Jiang, J. Trends in anthropogenic mercury emissions in China from 1995 to 2003. *Environ. Sci. Technol.* **2006**, *40*, 5312–5318.

(31) Wu, Y.; Streets, D. G.; Wang, S. X.; Hao, J. M. Uncertainties in estimating mercury emissions from coal-fired power plants in China. *Atmos. Chem. Phys.* **2010**, *10*, 2937–2947.

(32) Grübler, A.; Nakicenovic, N.; Victor, D. G. Dynamics of energy technologies and global change. *Energ. Policy* **1999**, *27*, 247–280.

(33) Riahi, K.; Rubin, E. S.; Taylor, M. R.; Schrattenholzer, L.; Hounshell, D. Technological learning for carbon capture and sequestration technologies. *Energy Econ.* **2004**, *26*, 539–564.

(34) Nakicenovic, N. The automotive road to technological change: Diffusion of the automobiles as a process of technological substitution. *Technol. Forecast. Soc.* **1986**, *29*, 309–340.

(35) *Mercury Study Report to Congress: An Inventory of Anthropogenic Mercury Emissions in the United States*, Report EPA-452/R-97-004; U.S. Environmental Protection Agency: Washington, DC, 1997; Vol. II.
(36) *Assessment of Mercury Releases from the Russian Federation*, Arctic Council Action Plan to Eliminate Pollution of the Arctic (ACAP); Danish Environmental Protection Agency: Copenhagen, Denmark, 2005.
(37) *Air Pollutant Emission Inventory Guidebook*; European Environment Agency: Copenhagen, Denmark, 2009.
(38) Hylander, L. D.; Herbert, R. B. Global emission and production of mercury during the pyrometallurgical extraction of nonferrous sulfide ores. *Environ. Sci. Technol.* **2008**, *42*, 5971–5977.
(39) Pirrone, N.; Allegrini, I.; Keeler, G. J.; Nriagu, J. O.; Rossmann, R.; Robbins, J. A. Historical atmospheric mercury emissions and depositions in North America compared to mercury accumulations in sedimentary records. *Atmos. Environ.* **1998**, *32*, 929–940.
(40) Strode, S.; Jaeglé, L.; Selin, N. E. Impact of mercury emissions from historic gold and silver mining: Global modeling. *Atmos. Environ.* **2009**, *43*, 2012–2017.
(41) Hylander, L. D.; Meili, M. The rise and fall of mercury: Converting a resource to refuse after 500 years of mining and pollution. *Crit. Rev. Env. Sci. Technol.* **2005**, *35*, 1–36.
(42) Lacerda, L. D. Global mercury emissions from gold and silver mining. *Water, Air, Soil Pollut.* **1997**, *97*, 209–221.
(43) Nriagu, J. O. Legacy of mercury pollution. *Nature* **1993**, *363*, 589.
(44) Nriagu, J. O. Mercury pollution from the past mining of gold and silver in the Americas. *Sci. Total Environ.* **1994**, *149*, 167–181.
(45) Camargo, J. A. Contribution of Spanish-American silver mines (1570−1820) to the present high mercury concentrations in the global environment: A review. *Chemosphere* **2002**, *48*, 51–57.
(46) Cooke, C. A.; Balcom, P. H.; Biester, H.; Wolfe, A. P. Over three millennia of mercury pollution in the Peruvian Andes. *Proc. Natl. Acad. Sci. U.S.A.* **2009**, *106*, 8830–8834.
(47) Slemr, F.; Brunke, E.-G.; Ebinghaus, R.; Kuss, J. Worldwide trend of atmospheric mercury since 1995. *Atmos. Chem. Phys.* **2011**, *11*, 4779–4787.
(48) Ebinghaus, R.; Jennings, S. G.; Kock, H. H.; Derwent, R. G.; Manning, A. J.; Spain, T. G. Decreasing trends in total gaseous mercury observations in baseline air at Mace Head, Ireland from 1996 to 2009. *Atmos. Environ.* **2011**, *45*, 3475–3480.
(49) Cole, A. S.; Steffen, A. Trends in long-term gaseous mercury observations in the Arctic and effects of temperature and other atmospheric conditions. *Atmos. Chem. Phys.* **2010**, *10*, 4661–4672.